ELSEVIER

Journal of Nuclear Materials 265 (1999) 225–231

journal of nuclear materials

The effect of hydrogen on the fracture toughness of alloy X-750 at elevated temperatures

Douglas M. Symons

Bettis Atomic Power Laboratory, Westinghouse Electric Company, P.O. Box 79, West Mifflin, PA 15122, USA

Received 23 September 1998; accepted 18 November 1998

Abstract

Ni–Cr–Fe alloys are widely used in pressurized water nuclear reactors (PWR). These alloys are susceptible to stress corrosion cracking (SCC) in PWR environments. There have been numerous mechanisms of crack advance proposed to describe the SCC of the nickel-base alloys in a PWR environment including slip/film rupture/oxidation and hydrogen embrittlement. It has also been suggested that there is not sufficient evidence to implicate hydrogen in the PWR SCC of nickel-base alloys. This program evaluated the effect of hydrogen on the embrittlement of a nickel-base alloy, alloy X-750, at elevated temperatures with a hydrogen concentration typical of what may be developed from the corrosion reaction. Fracture toughness values and the tearing resistance of alloy X-750 were evaluated in hydrogen gas and in air 260°C and 338°C. It was shown that at 260°C and 338°C alloy X-750 was severely embrittled in high pressure hydrogen gas. Further, the fracture morphology changed from predominantly transgranular ductile dimple fracture in air to predominantly intergranular fracture in hydrogen. The fracture morphology in hydrogen was similar to that found for PWR SCC of this material. This work supports a hydrogen-enhanced fracture mechanism contributing to the SCC of nickel-base alloys at elevated temperatures.

1. Introduction

Ni–Cr–Fe alloys are widely used in pressurized water nuclear reactors (PWR) [1–3]. These materials are susceptible to environmental degradation in hydrogenated water environments. There are two phenomena associated with the degradation of the nickel-base alloys in a hydrogenated water environment: low temperature crack propagation (LTCP) and high temperature stress corrosion cracking (HTSCC). Many nickel-base alloys such as alloy X-750, alloy 690, EN82H (alloy 600 weld metal), and EN52 (alloy 690 weld metal) are susceptible to LTCP in hydrogenated water [2,4]. LTCP occurs at temperatures below 150°C and is characterized by precipitous drop in the fracture toughness of the material and rapid subcritical crack growth [2,4]. It has been shown that LTCP is a hydrogen-enhanced cracking phenomenon [2,4]. The HTSCC behavior of Ni-base alloys in high purity water has been well documented [1–3,5–7]. HTSCC has been observed between 250°C and 360°C. This phenomenon is characterized by a time to incubate the crack followed by a relatively low crack growth rate, on the order of 5×10^{-10} m/s in 360°C deaerated hydrogenated water, depending on the load. The mechanism of HTSCC continues to be controversial. It is important to understand the mechanism in order to develop a model capable of extrapolating to conditions in which tests cannot be run. The two most prevalent mechanisms for SCC of nickel-base alloys in PWR environments are based on slip/film rupture/oxidation [8] and hydrogen enhanced cracking [9–11].

While hydrogen has been shown to contribute to the embrittlement of materials in many instances, it has been suggested that hydrogen may not affect the fracture behavior of the Ni-base alloys at temperatures typical of commercial reactors [12]. The purpose of this program was to evaluate the effect of hydrogen on the embrittlement of a nickel-base alloy, alloy X-750, at elevated temperatures with hydrogen concentrations in the metal representative of those that may be generated from the corrosion process. Alloy X-750 is susceptible to both HTSCC and LTCP in pressurized water reactors [2,3].

The bulk hydrogen content has been measured in nickel-base alloys after constant extension rate test (CERT) in hydrogenated water with hydrogen overpressures of 0.005 to 0.1 MPa. In the area near the

0022-3115/99/$ – see front matter
PII: S0022-3115(98)00888-5

fracture surface of the CERT specimen, the measured hydrogen concentration was between 20 and 80 ppm by weight [9,13]. It should be noted that this hydrogen concentration is much higher than would be calculated using Sievert's law for the solubility of hydrogen in the metal that would be in equilibrium with the 0.005 to 0.1 MPa hydrogen overpressures in water. In fact, for the 43 ppm hydrogen measured in the X-750 specimen by Yonezawa et al. [13], a hydrogen pressure of 20 MPa is required [14]. To achieve local hydrogen pressures this high, the hydrogen must come from the local corrosion reaction on the specimen. Therefore, while suggesting that the mechanism of cracking is hydrogen embrittlement, the local corrosion reaction is required to generate sufficient hydrogen to embrittle the material.

The analysis of the equilibrium pressure from the CERT testing assumes that the material in the fracture region is in equilibrium with the surface hydrogen concentration produced from the corrosion reaction. There are two paths for hydrogen transport through the specimen. The first is by bulk diffusion and the second is by dislocation transport [15]. The test time for the X-750 specimen tested at 360°C was 40 h. The diffusivity of hydrogen at 360°C is 1.4×10^{-10} m^2/s [14]. According to Crank, the test time required to achieve a near uniform hydrogen distribution through the thickness for these conditions is 15 h [16]. Therefore, while dislocation transport may reduce this time, it is not required to account for the high bulk hydrogen concentration measured.

Fracture toughness values and tearing resistance of condition HTH alloy X-750 were evaluated in hydrogen gas with 38 ppm hydrogen in the metal and in air with no hydrogen at 260°C and 338°C. 38 ppm hydrogen was used in this experiment to remain in the middle of the range of measurements of hydrogen in Ni–Cr–Fe alloys under going SCC in hydrogenated water [9,13].

It was shown that at 260°C and 338°C alloy X-750 was severely embrittled in the hydrogen gas environment. K_{IC} was decreased by over a factor of three. The tearing modulus was decreased from over 80 to very low values in the hydrogen environment. The fracture morphology was also changed from a predominantly transgranular ductile dimple morphology to predominantly intergranular fracture with some transgranular fracture facets. The hydrogen-induced intergranular fracture morphology is very similar to the fracture morphology observed on SCC specimens.

2. Experimental procedure

2.1. Materials

The material used in this program was a 6.35 cm diameter alloy X-750 bar heat treated to the HTH condition with the chemical composition given in Table 1. The HTH condition consists of a solution anneal at 1094°C for 1–2 h with a rapid air cool followed by again at 704°C for 20 h. The HTH microstructure has previously been characterized [17]. The mean intercept grain size of this heat was 125 μm with small discrete $M_{23}C_6$ carbide precipitates decorating the grain boundaries. The alloy was strengthened by ~20 nm γ' precipitates with a rounded cuboidal shape and a weight fraction of 0.126. Primary carbides and carbonitrides, M(C, N), were aligned along the rolling direction.

2.2. Fracture toughness testing

Compact tension specimens were machined out of the X-750 bar in the *L–R* orientation. The specimens had a thickness of 15.2 mm and a width of 30.5 mm. All specimens had side (face) grooves of 10% of the thickness per face. The specimens were side grooved prior to the precracking. This resulted in very little tunneling during precracking. The side grooves were essential to obtaining valid results since this material tends to have excessive tunneling. Even with the side grooves, the air test specimens showed slightly more tunneling than allowed per ASTM E-813. All specimens were precracked with a final K_{max} of 20 MPa$\sqrt{m}$ and an average normalized crack length (a/W) between 0.55–0.60. The test temperatures were 260°C and 338°C in both air and hydrogen gas. The testing in the hydrogen gas was performed at a hydrogen pressure of 13.8 MPa. The testing was performed in the gas environment to avoid hydrogen diffusing out of the crack tip during the test thereby maintaining a high surface hydrogen concentration.

The specimens to be tested in the hydrogen gas environment were first hydrogen precharged to obtain a uniform hydrogen concentration. According to Crank [16], the time needed to achieve a near-uniform hydrogen concentration is determined when the dimensionless parameter, diffusivity multiplied by time and divided by one-half the thickness squared (Dt/l^2), is greater than 1.5. The diffusivity is given by $D_H = D_0 \exp(-Q/RT)$ where $D_0 = 0.016$ cm^2/s, $Q = 49{,}000$ J/mol, R is in J/mol, T is in Kelvin, and D_H is in cm^2/s [14]. The minimum time required is calculated to be 11 days as compared to the 30 days used in this experiment. The hydrogen charging pressure was 13.8 MPa. Hydrogen blanks were also included in the autoclave. These blanks were analyzed for hydrogen concentration at the end of the test. The hydrogen concentration was determined to be 38 ppm. Following the charging, the specimens were stored in dry ice until required for testing.

One fracture toughness test was run per condition. The test sequence began by inserting the specimen into the autoclave once the specimen reached ambient temperature. The autoclave was then evacuated, back filled

Table 1
Chemical analysis (wt%)

Ni	Cr	Nb	Ti	Al	Fe	C	B
71.17	15.46	1.00	2.67	0.76	8.33	0.072	0.006
Mn	Si	S	Co	P	V	As	Cu
0.10	0.11	.001	0.07	0.007	0.02	<10 ppm	0.01

with high purity hydrogen, and taken to the test temperature. The specimen precrack was then extended a minimum of 0.25 mm in the environment and the specimen was held for a minimum of 24 h at temperature and pressure. The fracture toughness test was then run and analyzed according to ASTM E813-89 (Standard Test Method for J_{IC}, A Measure of Fracture Toughness), though for the specimens in the hydrogen atmosphere, the specimens were analyzed per ASTM E399 due to the severe embrittlement. Crack extension was determined by using the compliance technique. The compliance was measured using a capacitance based displacement gage attached to the front face of the specimen. This technique was used for the complete air tests and was used until the rapid subcritical crack advance occurred for the tests in hydrogen gas.

3. Results

The load displacement curves for alloy X-750 in hydrogen gas and air at elevated temperatures are shown in Fig. 1. It is observed that the specimens tested in the hydrogen gas behave in a near linear-elastic fashion. The compliance measurements show that the deviation from linear elasticity was due to subcritical crack growth, not plasticity. Further support for the deviation not being due to plasticity is that the specimens tested in air were still linear in this load regime. If the deviation was due to plasticity and not crack extension, it would be expected that the hydrogen test would behave in a similar manner to the air test. Therefore, it was possible to analyze the hydrogen gas tested specimens per the K_{IC} standard (ASTM E399-90). These specimens could be considered marginally valid per ASTM E399. The size criterion was not quite met, 2.5 $(K_{IC}/\sigma_y)^2$ was 0.021 m for the 260°C test and 0.035 m for the 338°C test, though the specimens behaved in a brittle manner. The J-resistance curves in air and hydrogen at elevated temperatures are displayed in Fig. 2. The analysis of the data is shown in Table 2. The yield strength of this material at 260°C and 338°C tested at a strain rate of 3.33×10^{-4}/s is also given in Table 2. These results show that alloy X-750 is severely embrittled by hydrogen at elevated temperatures. At 260°C, K_{JC} is reduced from 220 MPa$\sqrt{m}$ to 68 MPa$\sqrt{m}$ while at 338°C K_{JC} is reduced from 230 to 87

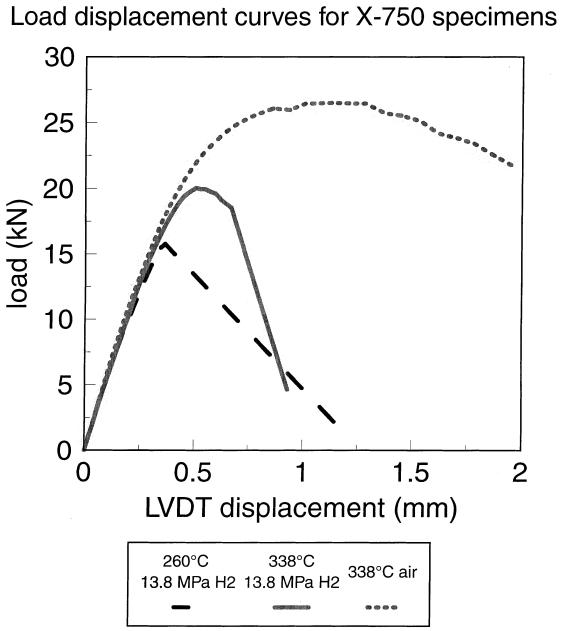

Fig. 1. Load displacement curves for alloy X-750 specimens.

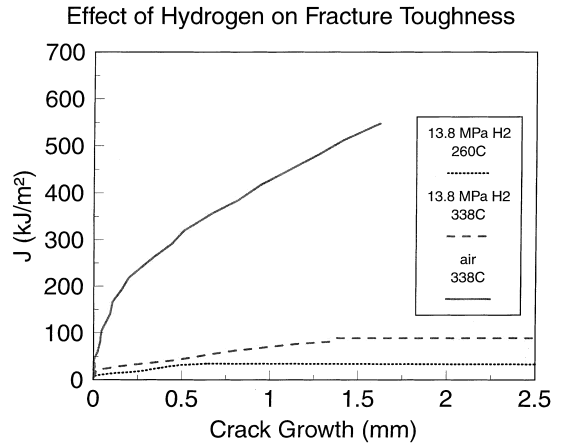

Fig. 2. Effect of hydrogen on fracture toughness.

MPa$\sqrt{m}$. At 260°C, once the maximum load was achieved in the hydrogen atmosphere testing, rapid stable crack growth was observed. At 338°C, rapid crack

Table 2
Fracture toughness properties of alloy X-750

Environment	Temperature (°C)	J_{IC} (kJ/m^2)	K_{JC} (MPa$\sqrt{m}$)	K_{IC} (MPa$\sqrt{m}$)	Tearing modulus	Yield stress (MPa)
Air	260	229	220	–	87	738
Air	338	252	230	–	82	728
H_2 gas	260	19	–	68	10	738
H_2 gas	338	30	–	87	11	728

growth was not observed until slightly after the maximum load was achieved.

The tearing modulus was evaluated for the specimens using the following equation, $T = (\mathrm{d}J/\mathrm{d}a) * (E/\sigma_f^2)$, where E is the elastic modulus at the test temperature, σ_f is the flow stress at the test temperature, and $\mathrm{d}J/\mathrm{d}a$ was the slope of the J–R curve between the 0.2 mm offset line and the 1.5 mm exclusion line. The tearing moduli were in the 80s for the specimens tested in air and were approximately 10 for the specimens tested in hydrogen gas. It should be noted that the resistance to the crack extension in the hydrogen atmosphere may be controlled by multiple factors including hydrogen diffusion to the high stress region and crack tip strain in the presence of hydrogen. Previous work on uniaxial specimens showed that plasticity is required in the presence of hydrogen for embrittlement of alloy X-750 [17].

The loss in fracture toughness due to the hydrogen environment was accompanied by a change in fracture morphology. The fracture morphology of the specimens tested in air was a transgranular ductile dimple morphology as shown in Fig. 3. The fracture morphology for the specimens tested at 260°C and 338°C in hydrogen are shown in Figs. 4 and 5, respectively. In the gas environment, the fracture morphology changed to a predominantly intergranular morphology with some transgranular faceted fracture. At 338°C there was more faceted transgranular fracture than at 260°C. For comparison, the fractography of a precracked compact tension specimen from the same heat of material tested at 360°C in hydrogenated water is shown in Fig. 6. The specimen tested in the water environment is also predominantly intergranular with small amounts of transgranular faceting. The fractorgraphic features of the

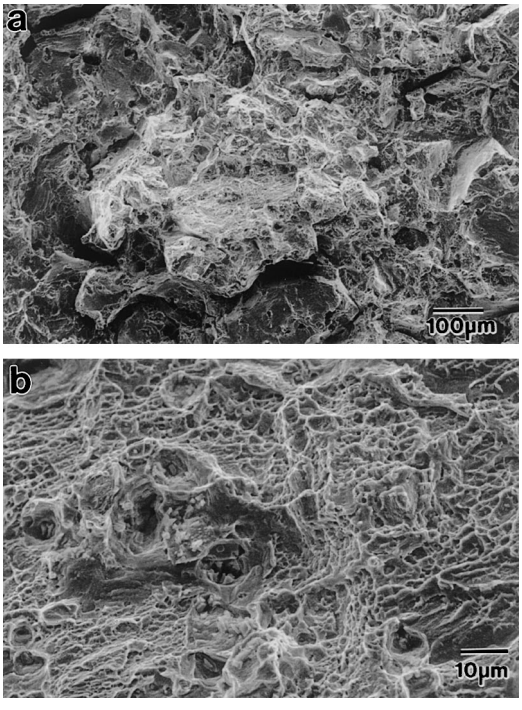

Fig. 3. (a) and (b) Fracture surface of specimen tested in air at 338°C.

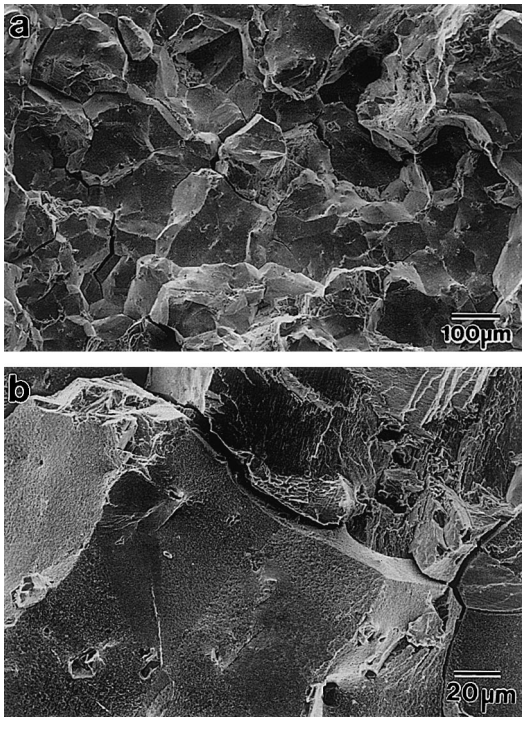

Fig. 4. (a) and (b) Fracture surface of specimen tested in hydrogen gas at 260°C.

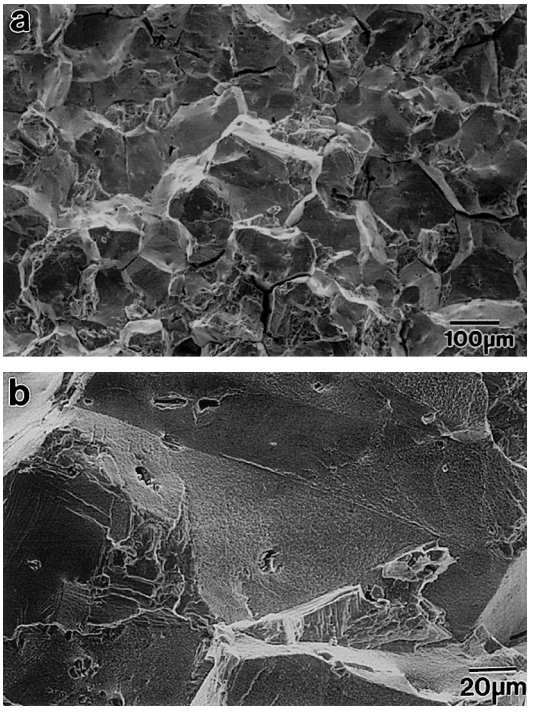

Fig. 5. (a) and (b) Fracture surface of specimen tested in hydrogen gas at 338°C.

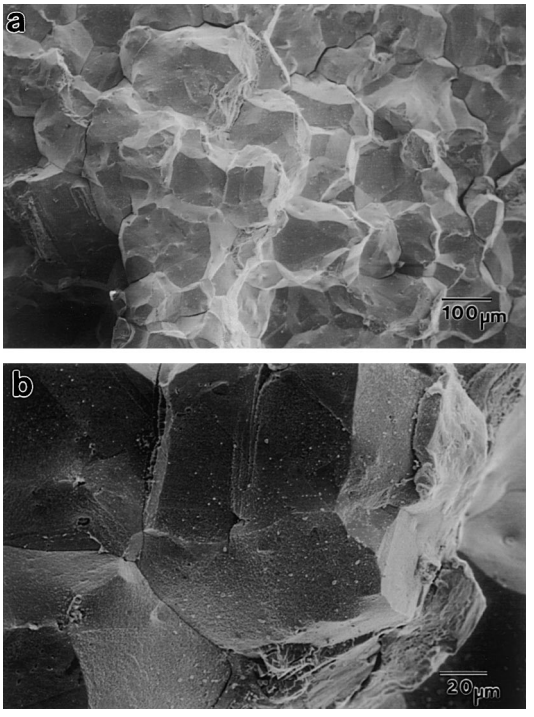

Fig. 6. (a) and (b) Fracture surface of specimen tested in hydrogenated water at 360°C.

SCC specimen are very similar to the specimens tested in hydrogen gas.

4. Discussion

The hydrogen embrittlement of nickel-base alloys at temperatures below 150°C is well accepted [18]. It is further accepted that the mechanism of low temperature crack propagation of nickel-base alloys (alloy 690 and alloy X-750) in hydrogenated water is hydrogen embrittlement [4]. It has been suggested that hydrogen may not affect the fracture behavior of the Ni-base alloys at temperatures prototypic of commercial reactors [12]. This work shows that hydrogen severely embrittles one of the nickel-base alloys used in PWR at elevated temperatures.

It has been proposed that the effect of hydrogen on the behavior of alloy X-750 is either to reduce the strength of the interface between the matrix and the grain boundary carbides or to enhance local plasticity [17,19]. The reduction in the interfacial strength or enhanced local plasticity near the grain boundary would result in a lower macroscopic strain required for the initiation of a microcrack. Lassila and Birmbaum showed that the key parameter to describe the degree of embrittlement in Ni is the grain boundary hydrogen concentration [20]. Lassila and Birnbaum aged hydrogen charged tensile specimens to allow for the diffusive segregation of hydrogen then tested the specimens at a temperature where no additional diffusion could occur thereby allowing the critical hydrogen concentration to be determined along with the trapping energy of hydrogen at the grain boundaries. A similar methodology was used to examine the fracture behavior of the specimens tested in this program. Two additional aspects must be incorporated into the analysis of fracture mechanics specimens of engineering alloys: (1) the role of the hydrostatic stress ahead of the crack increasing local hydrogen solubility; and (2) the increased trapping of hydrogen at grain boundaries due to carbide precipitation. In order to determine if these results are consistent with the previous results of Lassila and Birnbaum, the concentration of trapped hydrogen at the grain boundaries will be compared with the critical hydrogen of the tensile specimens [20].

The hydrostatic stress increases the distance between matrix atoms, thereby increasing the local solubility of hydrogen. The equation that describes the effect of stress on the hydrogen distribution ahead of the crack is [21]

$$C_{\mathrm{H}_\sigma} = C_{\mathrm{H}} \exp\left(\frac{\sigma_{\mathrm{H}} \bar{V}}{RT}\right), \tag{1}$$

where C_{H_σ} is the local hydrogen concentration in the crack tip stress field, C_{H} is the hydrogen concentration in

the unstressed region, σ_H is the hydrostatic stress, $\bar{V}$ is the partial molar volume of hydrogen, R is the universal gas constant and T is the absolute temperature in Kelvin. The partial molar volume was taken to be 1.72 cm^3/mol [22].

The stress field ahead of a crack may be described by Rice and Johnson's analysis of cracks under large geometry change conditions from the tip to two crack tip opening displacements (CTODs) [23]. From Rice and Johnson's solution, the stress at the crack tip is four σ_y and at two CTODs it is five σ_y. The stress from two CTODs to 10 CTODs may be described using the solution developed by Hutchinson [24] and Rice and Rosengren (HRR) [25]. The HRR solutions show that after 2 CTODs, the stress is a decreasing function of distance ahead of the crack. Therefore, the maximum stress is that from the work of Rice and Johnson. The hydrostatic stress was determined by using the approximation of Akhurst and Baker [26]

$$\sigma_H = (2\sigma_{11} - \sigma_y)(1 + v)/3, \tag{2}$$

where σ_H is the hydrostatic stress, σ_y is the yield strength and v is Poisson's ratio. Incorporating Eq. (2) into Eq. (1) results in an increase in local hydrogen concentration due to the hydrostatic stress field of 3 at 260°C and 2.6 at 338°C.

Once the local matrix hydrogen concentration in the hydrostatic stress field is determined as just described, the grain boundary hydrogen level may be evaluated. The grain boundary concentration is dependent on the test temperature, matrix hydrogen content, and binding energy to the grain boundary. An expression for the equilibrium hydrogen concentration on the grain boundaries was developed by McLean [27] and is given in Eq. (3):

$$\frac{C_{GB}}{1 - C_{GB}} = \frac{C_{H_\sigma}}{1 - C_{H_\sigma}} \exp\left(\frac{H_B}{RT}\right), \tag{3}$$

where C_{GB} is the fraction of grain boundary sites that contain hydrogen, C_{H_σ} is the fraction of hydrogen solute in the matrix in the region of the hydrostatic stress, R is 8.314 J/mol K, H_B is the binding energy of hydrogen to grain boundaries in J, and T is the test temperature in Kelvin. Two binding energies will be used in the analysis of the grain boundary hydrogen concentration. The first is 12 kJ/mol as determined by the work of Lassila and Birnbaum [20]. This is the binding energy of hydrogen to grain boundary regions in clean Ni. This is a lower limit to the trapping of hydrogen to grain boundaries. The second possible binding energy is 26 kJ/mol as determined from thermal desorption studies by Young and Scully on alloy 600 [28]. The 26 kJ/mol corresponds to trapping on $M_{23}C_6$ type grain boundary carbides. This could be considered an upper bound for hydrogen trapped at the carbide matrix interface. It will be assumed that near the crack tip, the grain boundary hydrogen concentration is at equilibrium. Local equilibrium may be supported by diffusion calculations. The average diffusion distance by the end of the test (square root of $4Dt$) is over 350 μm while the fracture is expected to occur within the first 10 μm [19].

Table 3
Evaluation of the grain boundary hydrogen in alloy X-750

Test Temp. (°C)	GB Hydrogen (atoms H/atoms Ni)	
	$H_B = 12$ kJ/mol	$H_B = 26$ kJ/mol
260	0.09	0.7
338	0.06	0.5

The hydrogen concentrations on the grain boundaries for the two tests using the two different binding energies are shown in Table 3. Using the binding energy developed by Lassila and Birnbaum, the hydrogen concentrations in these specimens are consistent with the high degree of embrittlement observed. Lassila and Birnbaum showed that ~0.07 H/Ni was required for embrittlement. The binding energy of 26 kJ/mol resulted in a much higher hydrogen concentration than the 0.07 that Lassila and Birnbaum showed was required for the intergranular fracture of Ni. This work does not show which binding energy is more appropriate to analyze the current data, but it does show that both binding energies are consistent with the high degree of embrittlement observed. While hydrogen embrittlement of the nickel-base alloys is not commonly reported at these elevated temperatures, this work shows hydrogen embrittlement is possible under conditions where hydrogen levels are typical of those developed on specimens undergoing SCC. The similarities in the fracture morphologies between the specimens tested in hydrogen gas and hydrogenated water further support the mechanism of SCC being related to hydrogen embrittlement.

5. Summary

1. Hydrogen reduces the fracture toughness of alloy X-750 at elevated temperatures. At 260°C K_{JC} is reduced from 220 to 68 MPa$\sqrt{m}$ while at 338°C K_{JC} is reduced from 230 to 87 MPa$\sqrt{m}$.
2. At 260°C, once the maximum load was achieved in the hydrogen atmosphere testing, rapid stable crack growth was observed. At 338°C, rapid crack growth was not observed until slightly after the maximum load was achieved.
3. The tearing moduli were in the 80s for the air testing and near 10 for the testing in hydrogen gas. This shows that the materials resistance to crack advance is dramatically reduced by hydrogen.
4. The fractographic features are very similar between specimens tested in a high-pressure hydrogen gas and tested in hydrogenated water.

5. This work suggests that hydrogen may play a key role in the embrittlement of nickel-base alloys in high temperature water environments.

Acknowledgements

This work was supported under US DOE Contract DE-AC-93PN38195 with Bettis Laboratory. The hydrogen gas testing was performed at Materials Engineering Associates. I would like to thank Dr M. M. Hall for the many fruitful discussions on relating the hydrogen gas work to experiments performed in a high temperature water environment.

References

[1] P. Berge, Experience with alloy X-750 in PWR's, in: Proceedings: 1986 Workshop on Advanced High Strength Materials, EPRI NP-6363.
[2] C.A. Grove, L.D. Petzold, Corrosion of Nickel-Base Alloys, ASM, Mars, PA, 1985, p. 165–180.
[3] D.L. Baty, G.O. Hayner, G.S. Clevinger, Metallurgical factors affecting the failure of alloy X-750 hold down pins, in: International Symposium of Environmental Degradation of Materials in Nuclear Power Systems-Water Reactors.
[4] C.M. Brown, W.J. Mills, Fracture toughness, tensile, and stress corrosion cracking properties of alloy 600, alloy 690, and their welds in water, Paper #90, Corrosion 90, NACE.
[5] J.P. Foster, W.H. Bamford, R.J. Panthania, in: Seventh International Symposium on Environmental Degradation of Materials in Nuclear Power Systems-Water Reactors, NACE, August 1995, pp. 25–40.
[6] G.L. Webb, in: R.E. Gold, E.P. Simonen (Eds.), Sixth International Symposium on Environmental Degradation of Materials in Nuclear Power Systems – Water Reactors, TMS, Warrendale, PA, 1993, pp. 687–695.
[7] M.O. Speidel, R. Magdowski, in: R.E. Gold, E.P. Simonen (Eds.), Sixth International Symposium on Environmental Degradation of Materials in Nuclear Power Systems-Water Reactors, TMS, Warrendale, PA, 1993, pp. 361–371.
[8] P.L. Andresen, F.P. Ford, Mater. Sci. Eng. A103 (1988) 167.
[9] N. Totsuka, E. Lunarska, G. Cragnolino, Z. Szklarska-Smialowska, Corrosion 43 (8) (1987) 505.
[10] J. Lagerström, U. Ehrnstén, T. Saario, T. Laitnen, H. Hänninen, Model for environmentally assisted cracking alloy 600 in PWR water, in: Eighth International Symposium of Environmental Degradation of Materials in Nuclear Power Systems – Water Reactors, Amelia Island, Fl, 11–14 August 1997, pp. 349–356.
[11] M.M. Hall Jr., Thermally activated dislocation creep model for primary water stress corrosion cracking of Ni-Cr-Fe alloys, in: T. Shoji, T. Shibata (Eds.), Proceedings of International Symposium of Plant Aging and Life Prediction of Corrodible Structures, NACE, 1997, pp. 107–116.
[12] P. Andresen, T.M. Angeliu, Evaluation of the Role of Hydrogen in SCC in Hot Water, CORROSION 97, NACE, TX, 1997, paper 195.
[13] T. Yonezawa, Y. Yamaguchi, Y. Iijima, Electron micro autoradiographic observation of tritium distribution on alloy X-750, in: R.E. Gold, E.P. Simonen (Eds.), Sixth International Symposium of Environmental Degradation of Materials in Nuclear Power Systems – Water Reactors, TMS, 1993, pp. 799–804.
[14] D.M. Symons, PhD dissertation, Carnegie Mellon University, Pittsburgh, PA, November 1994.
[15] S.V. Nair, R.R. Jensen, J.K. Tien, Metall. Trans. 14A (1983) 385–393.
[16] J. Crank, Mathematics of Diffusion, Clarendon, Oxford, 1956.
[17] D.M. Symons, A.W. Thompson, Met. Mater. Trans. A 27A (1996) 101.
[18] A.W. Thompson, I.M. Bernstein, in: M.G. Fontana, R.W. Staehle (Eds.), Advances in Corrosion Science and Technology, vol. 7, Plenum, New York, 1980.
[19] D.M. Symons, A.W. Thompson, The effect of hydrogen on the fracture toughness of alloy X-750, Met. Mater. Trans. (1997) pp. 817–824.
[20] D.H. Lassila, H.K. Birnbaum, Acta Metall. 36 (10) (1988) 2821–2825.
[21] J.C.M. Li, R.A. Oriani, L.S. Darken, Z. Phys. Chem. (N.F.) 49 (1966) 271.
[22] B. Baranowski, S. Majchrzak, T.B. Flanagan, J. Phys. F: Metal Physics 1 (1971) 258.
[23] J.R. Rice, M.A. Johnshon, in: M.F. Kanninen (Eds.), Inelastic Behavior of Solids, McGraw-Hill, New York, 1970, p. 641.
[24] J.W. Hutchinson, J. Mech. Phys. Solids 16 (1968) 13.
[25] J.R. Rice, G.R. Rosengren, J. Mech. Phys. Solids 16 (1968) 1–12.
[26] K.N. Akhurst, T. N Baker, Metall. Trans. A 12A (1981) 1059–1070.
[27] D. McLean, Grain Boundaries in Metals, Oxford University, Oxford, 1957.
[28] G.A. Young, J.R. Scully, Scripta Mater. 36 (1997) 713.